4-19-2016

Total- and Monomethyl-Mercury and Major Ions in Coastal California Fog Water: Results from Two Years of Sampling on Land and at Sea

Peter Weiss-Penzias

Kenneth Coale

Wesley Heim

Daniel Fernandez
California State University, Monterey Bay, dfernandez@csumb.edu

Andrew Oliphant

See next page for additional authors

ELEMENTA
Science of the Anthropocene

Total- and monomethyl-mercury and major ions in coastal California fog water: Results from two years of sampling on land and at sea

Peter Weiss-Penzias[1*] • Kenneth Coale[2] • Wesley Heim[2] • Daniel Fernandez[3] • Andrew Oliphant[4] • Celeste Dodge[5] • Dave Hoskins[6] • James Farlin[7] • Robert Moranville[1] • Alex Olson[2]

[1]University of California, Santa Cruz, California, United States
[2]Moss Landing Marine Laboratories, Moss Landing, California, United States
[3]California State University, Monterey Bay, Seaside, California, United States
[4]California State University, San Francisco, California, United States
[5]Pepperwood Preserve, Santa Rosa, California, United States
[6]California State University, Humboldt, Arcata, California, United States
[7]University of California, Davis, California, United States

*pweiss@ucsc.edu

Abstract

Marine fog water samples were collected over two summers (2014–2015) with active strand collectors (CASCC) at eight coastal sites from Humboldt to Monterey counties in California, USA, and on four ocean cruises along the California coastline in order to investigate mercury (Hg) cycling at the ocean-atmosphere-land interface. The mean concentration of monomethylmercury (MMHg) in fog water across terrestrial sites for both years was 1.6 ± 1.9 ng L^{-1} (<0.01–10.4 ng L^{-1}, N = 149), which corresponds to 5.7% (2.0–10.8%) of total Hg (HgT) in fog. Rain water samples from three sites had mean MMHg concentrations of 0.20 ± 0.12 ng L^{-1} (N = 5) corresponding to 1.4% of HgT. Fog water samples collected at sea had MMHg concentrations of 0.08 ± 0.15 ng L^{-1} (N = 14) corresponding to 0.4% of HgT. Significantly higher MMHg concentrations in fog were observed at terrestrial sites next to the ocean relative to a site 40 kilometers inland, and the mean difference was 1.6 ng L^{-1}. Using a rate constant for photo-demethylation of MMHg of -0.022 h^{-1} based on previous demethylation experiments and a coastal-inland fog transport time of 12 hours, a mean difference of only 0.5 ng L^{-1} of MMHg was predicted between coastal and inland sites, indicating other unknown source and/or sink pathways are important for MMHg in fog. Fog water deposition to a standard passive 1.00 m^2 fog collector at six terrestrial sites averaged 0.10 ± 0.07 L m^{-2} d^{-1}, which was ~2% of typical rainwater deposition in this area. Mean air-surface fog water fluxes of MMHg and HgT were then calculated to be 34 ± 40 ng m^{-2} y^{-1} and 546 ± 581 ng m^{-2} y^{-1}, respectively. These correspond to 33% and 13% of the rain fluxes, respectively.

1.0 Introduction

Mercury (Hg) pollution in the environment is a global concern due to its neurotoxicity in humans (especially in utero) and wildlife, and its ability to biomagnify and bioaccumulate as monomethylmercury (MMHg) (Mergler et al., 2007; Scheuhammer et al., 2007). The Minimata Convention, signed by 128 countries, states as its objective to "protect human health and the environment from anthropogenic emissions and releases of mercury and mercury compounds" (UNEP Minamata Convention, 2014). One of the difficulties in assessing the effectiveness of this global agreement is that more research is needed to elucidate mechanisms of Hg cycling between the atmosphere, deposition to the earth's surface, and accumulation of MMHg in terrestrial and aquatic ecosystems (Driscoll et al., 2013; Pirrone et al., 2013).

Domain Editor-in-Chief
Joel D. Blum, University of Michigan

Guest Editor
Anne Soerensen, Stockholm University

Knowledge Domains
Atmospheric Science
Ocean Science

Article Type
Research Article

Part of an *Elementa* Special Feature
Monitoring, measuring and modeling atmospheric mercury and air-surface exchange – are we making progress?

Received: November 30, 2015
Accepted: March 11, 2016
Published: April 19, 2016

Mercury is a highly unusual metal since it exists as a free atom in the gas phase and it is relatively long-lived in the atmosphere with a lifetime of gaseous elemental Hg (Hg^0) of 6 months–2 years (Schroeder and Munthe, 1998). Hg^0 is distributed globally and the atmosphere is the main transport pathway to sensitive ecosystems far from anthropogenic and natural sources (Fitzgerald et al., 1998; Steffen et al., 2015; Shanley et al., 2015). Once oxidized in the atmosphere, Hg^0 converts to gaseous oxidized Hg (Hg^{II}) and particulate bound Hg^{II} which have much shorter atmospheric lifetimes (hours to days) and these species readily deposit to water and land surfaces (Lindberg et al., 2007). Newly deposited Hg is thought to be more likely to enter the food web over older mineral-bound Hg in soils, meaning that the atmospheric burden of Hg is critical in controlling the accumulation in aquatic ecosystems (Harris et al., 2007).

In addition to inorganic Hg in the atmosphere, organic forms of Hg^{II} also exist in gas, particulate and aqueous phases, but little is known about these species since concentrations are usually very low (Mason et al., 1992). Typically MMHg concentrations in rain water are about 1% of total Hg or about 0.15 ng L^{-1} (Bloom and Watras, 1989; Kieber et al., 2008). The formation of MMHg in precipitation is not well understood. Some research indicated that an abiotic mechanism involving the reaction between divalent Hg and the acetate ion or similar organic ligand could form MMHg (Gardfeldt et al., 2003; Hammerschmidt et al., 2007). Another study indicated that the photodecomposition of MMHg in rain water is likely faster than any abiotic MMHg formation reaction involving acetate (Bittrich et al., 2011).

The demethylation of dimethylmercury (DMHg) of aquatic origin may also lead to the formation of MMHg in precipitation (Munthe et al., 2001; St. Louis et al., 2005, 2007). Concentrations of DMHg were found to be generally low in surface ocean waters and were broadly distributed in deeper water suggesting the importance of *in situ* production (Mason et al., 2012). However, in certain biologically productive environments, DMHg concentrations in surface seawater were elevated. For example, in the Arctic under the sea ice, DMHg mean concentrations were 11.1 ± 4.1 pg L^{-1} (St. Louis et al., 2007) and in surface waters of the Monterey Bay during the spring coastal upwelling DMHg concentrations ranged from 12 to 58 pg L^{-1} (Conaway et al., 2009). DMHg, like elemental Hg, has low water solubility, whereas MMHg is much more soluble (Henry's Law solubility constants: DMHg = 1.55×10^{-3} mol m^{-3} Pa^{-1}, $Hg^0 = 1.37 \times 10^{-3}$ mol m^{-3} Pa^{-1}, MMHgCl = 6.3×10^4 mol m^{-3} Pa^{-1}) (Schroeder and Munthe, 1998). Using 20 pg L^{-1} for DMHg in surface seawater, a net instantaneous diffusive flux was calculated to be 0.035–0.95 ng m^{-2} hr^{-1} for wind speeds between 4–12 m s^{-1} (Black et al., 2009). Thus, the coastal atmosphere may contain a signal of DMHg of marine origin due to rapid demethylation in the gas phase involving halogen radicals (Niki et al., 1983). Conaway et al. (2010) investigated the MMHg concentration in rain water from 40 events during fall-winter-spring in Santa Cruz, California, on the coast of the Monterey Bay. However, in this study, low MMHg concentrations overall were found (0.14 ± 0.10 ng L^{-1}), with no seasonal variability that would have been indicative of seasonal DMHg evasion from ocean due to coastal upwelling. Subsequently, summertime marine fog water MMHg concentrations from samples collected in Santa Cruz, California were found to be enhanced (3.4 ± 3.8 ng L^{-1}, n = 8) relative to rain, with an apparent biotic source of MMHg associated with coastal upwelling (Weiss-Penzias et al., 2012). Similarly, MMHg of marine origin was found to accumulate in lichen on the coast of the Arctic Ocean (St. Pierre et al., 2015) and may represent a health risk to native populations who eat the caribou that feed off of the lichen.

Marine advective fog has been identified as a vector for distributing oceanic emissions of nitrogen species to upland locations in coastal Chile (Weathers et al., 2000). However, little is known about the ability of fog to transport chemicals from the Pacific Ocean to the coast of North America. In this region, fog is most prevalent between southern Oregon and central California (Koracin et al., 2014), which corresponds to the range of the redwood tree (*Sequoia sempervirens*) (Johnstone and Dawson, 2010). Fog water drip can make up a significant portion of the hydrologic inputs in a relatively narrow distance from the coast, and because of the Mediterranean climate where summer rainfall is scant, a great diversity of plant and animal species have evolved in this region that rely upon fog water inputs (Sawaske and Freyburg, 2015). Due to relatively high MMHg concentrations found in fog water (Weiss-Penzias et al., 2012), coastal terrestrial ecosystems may be vulnerable to food web Hg accumulations (Ortiz et al., 2014).

The goals of this project were to make measurements of MMHg and total mercury (HgT) in Pacific coast marine fog water samples taken from eight land stations and from four ship cruises in order to observe their spatial and temporal patterns and relationships to other major chemical species in fog water. Furthermore, we wanted to estimate the flux of these pollutants to the terrestrial ecosystem, and test our hypothesis that the main source of MMHg was marine in origin.

2.0 Methods

2.1 Terrestrial fog collection sites (FogNet)

Location and physical setting details of the eight terrestrial sites where fog water samples were collected for chemical analysis in the summers 2014–2015 are shown in Table 1. Standard operating procedures for this network of sites (termed "FogNet") were consistent. Four sites were within 0.2 km of the ocean, 3 sites

Table 1. Location and physical settings for terrestrial fog collection sites (FogNet)

Name	Site ID	Lat (°N)	Long (°W)	Elev (m)	Prevailing Wind Direction	Distance from Ocean (km)	Physical Setting within radius of 100 m
Humboldt State Marine Labs	HSU	41.06	124.15	20	NW	0.2	Ocean bluff, scrub brush,mixed conifer forest, lab/office buildings, houses.
Pepperwood Preserve	PPW	38.57	122.70	360	SW	40	Ridgetop with open fields and mixed evergreen forest, remote
Bodega Bay Marine Labs	BML	38.31	123.06	10	NW	0.05	Ocean bluff, scrub brush, grass, lab/office buildings, remote
San Fransicso State University	SFSU	37.72	122.48	150	NW	2	Rooftop of Thornton Hall, urban college campus
Montara Lighthouse	MTA	37.53	122.51	10	NW	0.1	Ocean bluff, prairie and scrub, buildings, CA Rt. 1
UC Santa Cruz	UCSC	37.00	122.06	240	S	5	Rooftop of ISB Labs, ~10 m below tree top in dense redwood/oak forest lab/office buildings
Long Marine Lab	LML	36.95	122.07	10	NW	0.02	Ocean bluff, chaparral, grass, lab/office buildings
Fritzche Field	FRF	36.70	121.76	40	NW	5	Chaparral and sand dunes, and agricultural fields and dirt

doi: 10.12952/journal.elementa.000101.t001

were 2–5 km away, and another site was 40 km from the ocean. Three pairs of sites were considered coastal-inland transects: 1) BML (coastal) and PPW (inland), 2) LML (coastal) and UCSC (inland), and 3) LML (coastal) and FRF (inland). All sites were located away from major sources of exhaust or roads in relatively pristine environments, and in areas with free air movement away from trees or tall structures. The exception was the SFSU site which was located in an urban rooftop setting. Each site was equipped with a Caltech Active Strand Cloudwater Collector (CASCC) and a passive Standard Fog Collector (SFC) located within 5 m of each other. The CASCC was maintained by the site operator daily in order to clean the collector in advance of a potential fog event. The passive collector was connected to a tipping bucket rain gauge and data logger, which recorded the volumes of fog water drip sampled by the 1.00 m^2 collector every 15 minutes. These data were downloaded about every 60 days. At all sites but one, the passive collector recorded 2 to 5 times more fog events than what was collected by the active collector. This demonstrated the efficiency of the 1.00 m^2 collector, especially at seaside locations where wind speeds were generally high. In contrast, the UCSC site which is a rooftop location 5 m below the forest canopy where winds were light, the active collector sampled 50% more events than were recorded by the passive collector. The majority of active collector fog water samples were from single fog events on a given day. During only five fog events, there were multiple samples collected, and these occurred at the PPW site. The times of day when fog water was most likely to be collected at each site were between midnight and 10:00 the next day, even though at sites nearest to the ocean, marine stratus clouds would persist throughout the day.

2.2 Fog water collector details

Fog water for chemical analysis was collected with a CASCC based on the design of Demoz et al. (1996). Seven CASCCs were built at the UCSC Machine Shop patterned after a CASCC from the Collett lab at Colorado State University (Figure S1). The body was built of 0.953 cm Lexan® held together with 316 stainless steel screws and airflow was generated by a 12V automobile cooling fan located downstream of the strands. The droplet collecting surfaces were made of Teflon® (strands, drip tray, drip tube) and the collection bottle used was an I-CHEM® 300-series 250 mL glass bottle with Teflon-lined polypropylene lid. Fittings holding the drip tube and bottle to the CASCC were made of Nylon. All materials used in the inlet portion of the CASCC were tested for their chemical inertness by analyzing rinse DI water for Hg content. The strand diameter and spacing dimensions were identical to those specified in Demoz et al. (1996). Air velocity at the strands was set at 8.0 m s^{-1}, slightly lower than the 8.5 m s^{-1} specified by Demoz et al. (1996) in order to mitigate excessive fan noise. The strand frames were made of 316 stainless steel and one set of three frames for the shipboard CASCC was coated with Dupont Teflon # 954-101 whereas all others were left uncoated. Doors made of Lexan® were attached to the collector by a brass hinge at the bottom and a plastic latch and pull solenoid at the top. A silicone rubber gasket was used where the door met the collector opening to minimize air and particle entry during non-foggy periods. Based on criteria defined

below, the system could engage the solenoids to lift the latches and allow the doors, which were set under tension with the hinges, to swing open and downward. At this time the fan would start pulling air through the strings to commence droplet coalescence. The CASCC was mounted on an aluminum surveyor's tripod which was securely anchored. The CASCC is capable of collecting a water sample during a rain event as well as fog and several rain events were sampled. With larger droplets, the limiting factor for collection is whether they make the turn into the collector. This depends on the drop size, wind speed, and the orientation of the collector with respect to the wind. To verify the inertness of the collector for Hg, data from the rain events were compared with data from a previous study where rain water was collected with an open funnel into a Teflon bottle (Conaway et al., 2010).

Automation of the door opening and fan on/off controls were accomplished with a Raspberry Pi® (RPi) model B 512 MB ram microcomputer and operating programs written in Python. The code (available at https://github.com/fogpi/FogPi) took readings from a Honeywell HumidIcon™ HIH-6130 for temperature (T) and relative humidity (RH), and counted pulses from a tipping bucket rain gauge (TBRG) (Spectrum Technologies), and an optical rain sensor (ORS) (RG-11, Hydreon Corp.). The RPi was connected via Ethernet cable to the internet through a static internet protocol address and this allowed for remote viewing of the collection bottle and door position with a webcam and real-time data and instrument status.

In the original work to quantify Hg in marine fog, the CASCC was set to turn on/off at fixed times of day (22:00–09:00 local time), since fog was regularly occurring at night and almost never of sufficient density to collect a sample during the day (Weiss-Penzias et al., 2012). However, this meant that the sampler could have been on for many hours before the onset of fog and thus may have accumulated gases and particles. Other studies of fog have typically employed an optical sensor to trigger the CASCC during a fog event (Carrillo et al., 2008 and references therein), however, for the present study these technologies were either not commercially available or too expensive to deploy at eight sites simultaneously. Thus, a simpler, cost-effective solution was sought, but not discovered until year two of the study. In year one the CASCC was triggered on/off using RH greater than a threshold, usually 90–93%, depending on the site. This method still allowed for the CASCC to be triggered many hours before the onset of the actual fog event and this must be kept in mind when interpreting the data. In year two of this study the TBRG and/or the ORS connected to the passive SFC were used in conjunction with the RH threshold to trigger the CASCC at two of the sites (FRF and PPW), which meant that the CASCC was activated when there were actual drops of water present (i.e. a wetting fog event). The remaining sites in year two used the RH-only triggering method. Admittedly, the use of different triggering methods between sites and years is a limitation in interpreting the data. However, at two sites (PPW and FRF) where RH-only triggering method was used in year 1 and the TBRG + RH threshold was used to trigger the CASCC in year 2, there were no significant differences in the mean concentrations of the Hg species measured from each year suggesting that the effect of the measurement method on the results presented is likely to be small.

The SFC consists of copper and galvanized pipe supporting a double layer of 1.00 m^2 35% Coresa Rachel shade mesh mounted vertically (Schemenauer and Cereceda, 1994) (Figure S2). The bottom of the collector stands 2 meters above the ground allowing sufficient airflow above, below, and around the collector. As wind and fog pass though the collector, water droplets form and they coalesce and fall to a collection tray. Water drains from the trough to a tipping bucket rain gauge connected to a 115 Watchdog data logger (Spectrum Technologies). Each tip of the rain gauge represents a volume of approximately 8 mL, with the actual calibration determined independently for each tipping bucket rain gauge, providing an accuracy of within 2%. A data logger records sums of tips over 15-minute intervals and has a storage capacity of approximately 3 months. Data logger batteries have an approximately one-year lifespan in the field. The amount of water collected by each fog collector is a representative measure of the fog water available at that site for deposition. The actual amount of fog water deposited is a function not only of the fog water available, but the degree to which it is intercepted by the flora. Fog, unlike rain, is transported primarily horizontally, so the interception of its droplets is highly dependent on the surface area and leaf characteristics provided by the foliar canopy (Juvik et al., 2011). All known days of rain were excluded from the data set, determined from local observations by the site operators and weather reports from the closest meteorology station in the National Weather Service. Between June and September in coastal California, rain events were rare and amounted to 4 days being excluded from the passive collector data set at HSU, 1 day at BML, 1 day at PPW, 1 day at LML, and 3 days at UCSC over the summers of 2014 and 2015.

2.3 Sampling, cleaning, preservation and storage procedures used at terrestrial sites

Standard clean techniques for collection of low-level aqueous Hg samples were followed at all times (USEPA, 2001, 2002), including using powder-free gloves when handling the sample jar and the active collector components. All site operators were instructed to collect a fog water sample if present (> 3 mL) in the morning no later than 10:00 local time, which limited the length of time the sample was exposed to sunlight. After sample collection the active components of the CASCC (strand frames, drip tray and drip tube) were cleaned with dilute soap solution and warm tap water followed by thorough rinsing with laboratory DI water.

Ultra-pure water (18 megaohm) was not available at all of the sampling sites. After cleaning of the CASCC, a field blank sample was obtained by spraying laboratory DI water across the strand frames with a garden spray bottle and collecting a field blank of about 150 mL in a sample jar. The CASCC was then reset by air drying the strands and closing the doors. Each site had a bucket of 10% HCl on hand in order to soak the strand frames, drip tray and drip tube for at least 1 hour, which was done every 30 days during each summer's campaign at each site. Both the fog sample and the field blank were treated identically; if the volume was > 50 mL then a 10 mL aliquot was removed into a polypropylene centrifuge tube and left unpreserved for future major ion analysis, and the remaining liquid was acidified to 0.4% with 12M HCl (Fisher Sci., Trace Metal Grade) for Hg analysis (Parker and Bloom, 2005). Liquid samples were stored refrigerated up to 1 month at each site. Aliquots were shipped in coolers with ice to the University of California, Santa Cruz (UCSC) for major ion analysis and the acidified samples to Moss Landing Marine Labs (MLML) for MMHg and HgT analysis. At MLML, MMHg analysis was done first on the acidified sample and, if enough sample remained, it was sent for HgT analysis. Therefore, if fog water samples were low volume (<40 mL), MMHg was the only analyte measured.

2.4 Sampling of fog water at sea

A CASCC was used to collect fog water samples at sea on three different UNOLS vessels over four separate cruises (Figure S3, S4). The intended purpose was to compare fog water sampled on land, vs fog water sampled at various locations along the continental margin and shelf regions where marine fog forms. Details on CASCC mounting configurations, operational methodologies and tactical sampling considerations for the at-sea fog water sampling during this program are described in the Supporting Information Text S2. There are many locations on a ship that can accommodate the CASCC as long as the bridge watch maintains the sampler upwind of the stacks at time of sampling. In our opinion, the deployment on the R/V *Point Sur* afforded the best separation between both bow-associated sea spray, and stack gases, yet, the integrity of the sample depended in large measure on the ship handling. Wind reversals between onshore flow during the afternoon, to an offshore flow late in the evening were common. Wind direction measurements were used to determine the apparent wind direction (the sum of the over-ground wind flow vector, plus the ship's vector). We tried to maintain at least a 90 degree separation between these vectors. If this could not be avoided, the bridge was instructed to shut down the sampling fan whose power switch was placed on the bridge. The duration of this sampling period can be on the order of hours, so we arranged our sampling plan to accommodate hydrographic and sediment sampling activities during the daytime, and fog sampling while steaming to the next station, during nighttime when fog was forming.

Standard clean techniques for collection of low-level aqueous Hg samples were followed at all times (USEPA, 2001, 2002). Prior to sampling with the sampling fan running, the active strand sampler was rinsed out with 10% HCl administered from a peristaltic pump using Teflon tubing and a plastic spray nozzle. In some cases the spray nozzle was affixed to a long fiberglass pole to reach the sampler deployed atop a sampling tower (R/V *Point Sur*), in other cases (R/V *Sproul* and *Oceanus*), it could be sprayed by hand directly into the opening of the sampler. Following the acid rinse, the sampler was rinsed with 18 megaohm Millipore Milli-Q water. After the MQ rinse, a sample of rinse water was taken as a sampling "blank" and a sample collection bottle was affixed to the sampler. Shipboard samples were kept refrigerated until preserved with HCl (0.4% v/v) generally within 24 hrs but not longer than 48 hrs from time of collection. Samples were transported to MLML and kept cool and in the dark prior to analysis for MMHg and HgT. While not sampling (during most daylight activities), the active strand sampler was typically bagged in plastic, with the doors shut.

2.5 Analytical details

For all fog, rain, and blank samples MMHg was analyzed at MLML following USEPA methods 1630 using Tekran® model 2700 cold-vapor atomic fluorescence spectrophotometry after distillation, and aqueous phase ethylation, and isothermal GC separation (Bloom, 1989; Horvat et al., 1993). All samples were analyzed within 6 months of collection (Parker and Bloom, 2005). Standard reference material (Dogfish muscle standard DORM-2), analytical duplicate, matrix spike recovery (MS), and matrix spike recovery duplicate (MSD) were analyzed for every 20 samples. Lab QA/QC data for 2015 are as follows: the mean recoveries of the reference materials were 95.7% (Dorm-2, n = 6). Spike recoveries averaged 88.4% (n = 23) and the mean relative percent difference (RPD) between spikes and spike duplicates was 8.6% (n = 13 pair). The mean RPD between analytical duplicates was 7.3% (n = 3 pairs). All instrument blanks were less than the method detection limit (MDL) of 0.011 ng L^{-1}, whereas field blanks were typically 0.03–0.08 ng L^{-1} for most samples as discussed below.

HgT concentrations in fog, rain, and blank samples was determined at MLML following USEPA method 1631 (Gill and Fitzgerald, 1987) and was carried out only when sufficient sample volume remained subsequent to MMHg analysis. The MDL was 0.20 ng L^{-1}, as determined by 3 times the standard deviation of replicate (n = 9) measurements of low level Hg spiked samples (0.40 ng L^{-1}). Fog samples and field blanks were never

below the MDL. The typical range for field blanks was 0.3–6 ng L^{-1}. Relative percent difference between duplicate sample bottles averaged 5.4% (n = 5), recovery of Hg spikes averaged 94.9% (n = 7), and recovery of reference material NIST 1641d averaged 97.0% (n = 4).

All analysis of samples and blanks for Hg species were done at MLML. As a check on the accuracy of these results, several fog water samples were analyzed at UC Santa Cruz for MMHg and HgT using the same methods outlined above (Figure S5, Figure S6). Results between the two labs agreed to within 22% and 14% for MMHg and HgT, respectively.

The major ions Cl^-, SO_4^{2-}, and NO_3^- were measured with an ion chromatograph with suppressed conductivity detection using 29 mM KOH eluent, quantified against standards made up from solid NaCl, Na_2SO_4, and KNO_3. An interlaboratory comparison was done between UC Santa Cruz and Harvey Mudd College for SO_4^{2-} and NO_3^- concentrations on two fog water samples and one field blank (Figure S7) and the two labs agreed to within 6% for both SO_4^{2-} and NO_3^-. Ammonium ion was determined with the salicylate method (#8155) using powder pillows (Hach Inc.). Standards were made from solid NH_4Cl.

2.6 Criteria for determining valid samples

Criterion 1 required that $[MMHg]_{blank}/[MMHg]_{fog\ sample} < 0.2$ for a blank-sample pair taken on the same day to ensure that the blank contamination was reasonably low. MMHg was used instead of HgT for this criterion because if the fog sample volume was < 40 mL only MMHg was determined. Criterion 2 required that the fog water sample volume was > 20 mL to prevent significant contribution from the rinse blank water since the design of the CASCC makes complete drying of all surfaces after rinse difficult. Of the 179 fog water samples collected at all terrestrial and ocean sites and analyzed for MMHg, 23 samples were removed due to criterion 1 (blank contamination) and 21 samples were removed due to criterion 2 (low total volume), and some were removed for both criteria leaving 149 valid samples. Concentrations of Hg species found in the blanks were not subtracted from fog water sample concentrations since, as explained below, it is thought that a significant portion of the blank originated from the fog water sample plus dry deposition, which were variable, and was not likely a contribution from the DI water nor the materials used to construct the CASCC.

Field blank concentrations of MMHg and HgT are shown in Table S1 and Figure S8. The mean blank concentration as a proportion of the mean fog sample concentration for MMHg and HgT was 0.07 and 0.12, respectively. In spite of this relatively low blank contribution overall, some blanks were high in both MMHg and HgT, especially at BML, and to a lesser extent at MTA and FRF. Blanks taken at HSU, PPW, UCSC, and LML had the lowest MMHg concentrations, and blanks at HSU, PPW, and UCSC had the lowest HgT concentrations. At these sites, there were only one or two field blanks exceeding criterion 1 over both years (Table S1). At BML, however, there was a significant correlation ($p = 0.03$) between the fog sample and the subsequent blank concentration of MMHg. Weather and sea state conditions at BML were the most extreme compared to the other sites, with the collector set up on the sea cliff and exposed to strong winds and sea spray. It is likely that the standard cleaning procedures were not sufficient at BML to remove the MMHg that accumulated in the CASCC from exposure to the fog and sea spray. The CASCC at the MTA site was also exposed to sea spray and could explain the higher blank values at that site, however FRF was 6 km inland yet nearly 40% of the blanks at this site exceeded criterion 1. At FRF, fog sample MMHg concentrations were lower than at the coast-side sites which meant that the blank concentrations also needed to be low in order to satisfy criterion 1. At each site, the DI water used for cleaning the CASCC had MMHg concentrations below the MDL. It is also unlikely that operator differences contributed to the blank differences between sites since at every site there were some blanks taken with MMHg concentrations < 0.1 ng L^{-1}. Future fog water sampling efforts with the CASCC may have to include daily acid cleaning in order to prevent build-up of Hg species on the surfaces.

In rain water, a linear relationship is often seen between log Hg concentration and precipitation volume due to the "washout" of soluble gases and particles in the atmosphere (Gratz et al., 2013; Lynam et al., 2014). All fog water samples (no criteria applied) were inspected for such a relationship and a significant linear correlation was seen for HgT but not for MMHg (Figure 1). For sample volumes < 20 mL there was a downturn in MMHg concentrations which is consistent with the potential contribution of DI rinse water to the low volume samples, indicating that criterion 2 was reasonable. Note that HgT analyses were not done on low volume samples (< 40 mL) due to insufficient sample remaining after analysis for MMHg.

2.7 Description of statistical methods

Data were organized using Microsoft Excel and Access. Plots were made and two-sample t-tests and linear regressions performed using Origin 2016. Maps were made with ArcGIS 10.3.1. The criteria for statistical significance in the difference between means or for a linear regression was met when the p-value < 0.05. Time trends in Hg species were determined for each site and for the data as a whole with the non-parametric

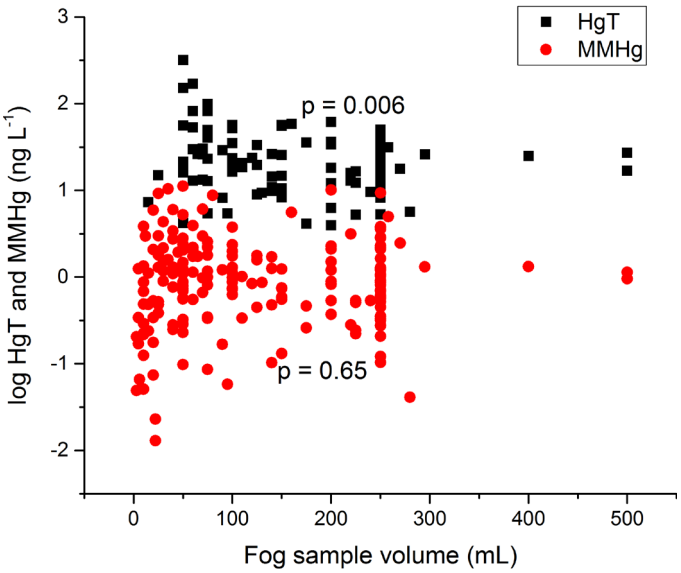

Figure 1

A scatter plot of the log of MMHg and HgT concentrations in fog water against the sample volume per event as collected by the CASCC at all terrestrial sites.

Sample jar capacity was 250 mL except in a few cases when a 500 mL jar was used. p-values are shown for linear fits of the data for each Hg species.

doi: 10.12952/journal.elementa.000101.f001

Mann-Kendall method which returns τ, the correlation coefficient and a p-value (Helsel et al., 2006). The input data for this analysis consisted of a decimal date and a concentration (daily mean was used for fog events with multiple samples).

3.0 Results and discussion

3.1 Comparison of 2014–2015 fog water Hg data with previous measurements

A summary of the concentrations of MMHg and HgT measured in fog water samples by site and by year is shown in Table 2. Median MMHg concentrations by terrestrial site and individual MMHg concentrations for each ship cruise site are shown in Figure 2. Box-whisker plots of MMHg and HgT concentrations for each terrestrial site and for all ship cruise sites combined, are shown in Figure 3. The mean ± 1σ concentration

Table 2. HgT and MMHg mean concentrations, standard deviations and number of valid fog water samples analyzed for sites listed from north to south with totals by year. Also shown is results for rain samples taken at HSU, UCSC, and LML

Site ID	Year(s)	Total Vol (L)	HgT (ng L^{-1})			MMHg (ng L^{-1})			%MMH g
			mean	σ	N	mean	σ	N	
HSU	2014–15	2.08	30.6	17.6	10	3.3	3.0	17	10.8
PPW[c]	2014–15	6.35	22.8	32.4	30	0.6	0.4	32	2.6
BML	2014–15	0.77	31.9	35.6	4	2.2	3.2	8	6.9
SFSU	2014–15	0.65	23.7	16.4	3	1.9	1.9	7	8.0
MTA	2014–15	0.37	34.2		1	2.6	1.6	5	7.6
UCSC	2014–15	6.78	25.9	16.5	35	1.7	2.0	44	6.6
LML	2014–15	1.22	27.8	15.7	8	1.5	0.9	15	5.4
FRF	2014–15	2.90	39.7	36.0	15	0.8	0.4	20	2.0
All Terrestrial	2014–15	22.0	27.6	25.8	107	1.6	1.9	149	5.8
All Terrestrial	2014	12.63	32.6[a]	29.5	63	1.9[b]	2.1	85	5.8
All Terrestrial	2015	8.46	20.4	17.3	44	1.2	1.5	64	5.9
All Ocean	2014–15	0.59	19.9	16.8	11	0.08	0.15	14	0.4
All Rain	2014–15	1.01	14.3	1.1	2	0.20	0.12	5	1.4

[a]2014 HgT concentration significantly higher than 2015 mean HgT concentration
[b]2014 MMHg concentration significantly higher than 2015 mean MMHg concentration
[c]Five fog events at PPW produced two samples each

doi: 10.12952/journal.elementa.000101.t002

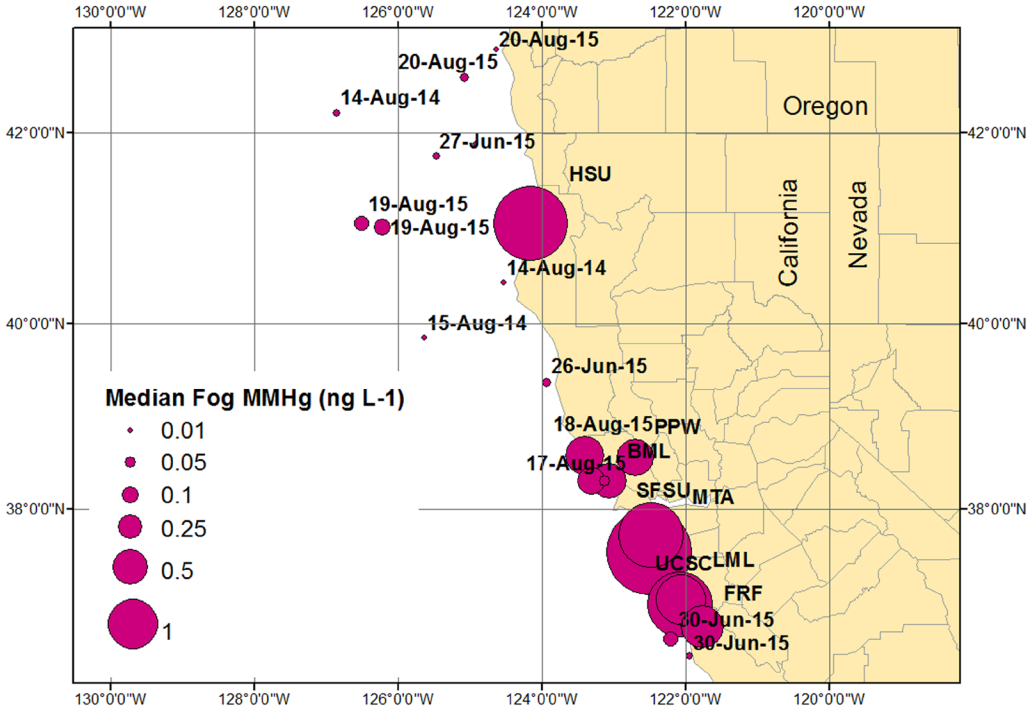

Figure 2

Land and ship cruise stations where fog samples were taken during the summers of 2014 and 2015, with symbols sized by MMHg concentration.

For the land stations, the symbols are the medians and for the ocean stations these are individual samples taken on the date shown. Ocean stations represent the approximate midpoint of the path of transit during fog collection.

doi: 10.12952/journal.elementa.000101.f002

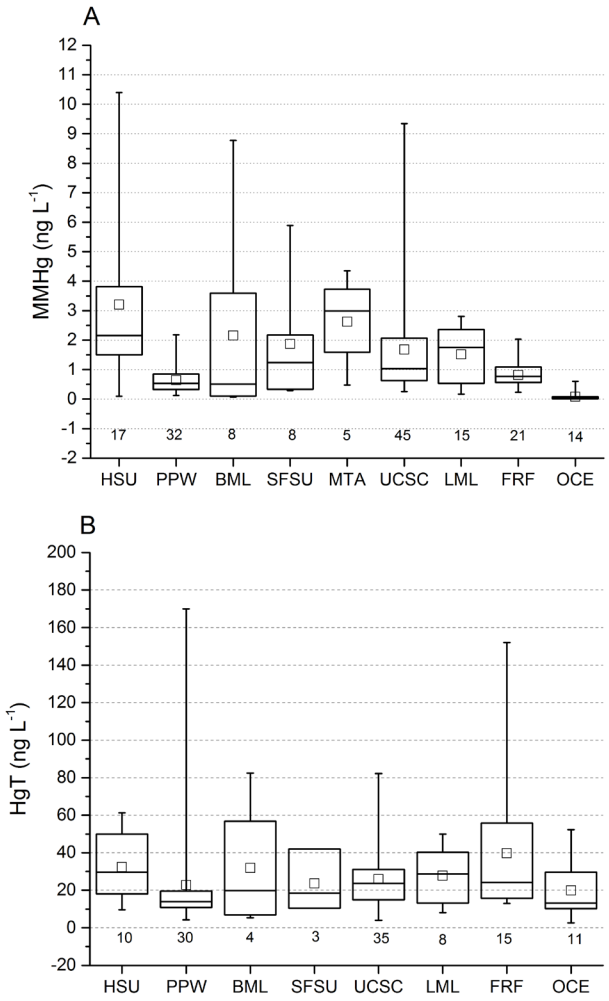

Figure 3

A) Monomethyl and B) total Hg concentration distributions in fog water from terrestrial sites in north to south order, plus the ocean sites (OCE) from 2014–2015.

The number of valid samples taken at each site is shown by numbers below the box. The boxes represent the lower and upper quartiles, the center line is the median, the square is the mean, and the whiskers are the minimum and maximum.

doi: 10.12952/journal.elementa.000101.f003

(range, number of samples) of MMHg in all valid fog samples across terrestrial sites for both years was 1.6 ± 1.9 ng L^{-1} (< 0.01–10.4 ng L^{-1}, N = 149) (Table 2). For comparison, rain water MMHg concentrations averaged 0.1 ± 0.1 ng L^{-1} in a previous study of rain collected with an open funnel on the coast of California (Conaway et al., 2010). Similarly low MMHg concentrations were observed in five rain samples that were collected with the CASCC at three terrestrial sites in this study (0.2 ± 0.1 ng L^{-1}) (Table 2). Thus, fog water mean MMHg concentrations in this study were approximately 10 times higher than MMHg concentrations typically found in rain water in this region.

The mean concentration of HgT across all terrestrial sites for both years was 27.8 ± 25.8 ng L^{-1} (0.9–170 ng L^{-1}, N = 108) (Table 2), resulting in mean %MMHg of 5.8% (range among site means: 2.0–10.8%). This is much lower than what was reported in the previous study (7–100%). One reason for this difference is that HgT concentrations reported here are higher than what was reported earlier (10.7 ± 6.8 ng L^{-1} N = 25) (Weiss-Penzias et al., 2012). We believe that the earlier work had HgT concentrations biased low due to sample digestion time with BrCl that lasted < 10 minutes instead of the > 3-hours sample digestion times used in the present work.

Fog water samples collected on four ship cruises had about an order of magnitude lower MMHg mean concentration (0.08 ± 0.15 ng L^{-1}, N = 14) compared to the samples that were collected at the terrestrial sites (Table 2, Figure 2, 3A). In contrast, mean HgT concentration in fog collected over the ocean (19.9 ± 16.8 ng L^{-1},) was not significantly different from mean HgT in fog at any of the terrestrial sites (Table 2, Figure 3B).

3.2 Spatial and temporal trends of MMHg, HgT and ions in fog water at terrestrial sites

Significant spatial trends in MMHg concentrations were observed across the terrestrial sites. The mean concentrations of MMHg were significantly higher at the sites right on the water's edge (HSU, BML, MTA, LML) compared to MMHg concentrations at PPW (40 km inland) (Table 2, Figure 2, 3). Also, the site at FRF (6 km inland) had significantly lower MMHg concentrations compared to the coastal site at LML. In contrast, significant spatial trends in the mean HgT concentrations were not observed between any two pairs of terrestrial sites.

A coastal-inland gradient was investigated by plotting the logs of Cl^-, MMHg, and HgT mean concentrations in fog water for each terrestrial site versus the log of distance from the site to the ocean (Figure 4). The ideal tracer of sea salt aerosol is the sodium ion, however, these data were not available. Chloride is then used here as a tracer of sea salt aerosol even though acid displacement reactions of sea salt chlorides with inorganic acids can lead to chlorine depletion of marine aerosols (Manders et al., 2010; Laskin et al., 2012). However, most chlorine depletion of aerosols has been observed in polluted air (Collett et al., 2002) or in aged aerosols (> 1 d) (Laskin et al., 2012), and these conditions did not apply to the sites in this study, where air mass transport times from the ocean were generally < 12 h and the locations were pristine. Even the urban site SFSU did not display elevated SO_4^{2-} or NO_3^- concentrations relative to other sites not at the ocean's edge (Table 3) indicating that pristine marine air was sampled at this site as well. According to Figure 4A, our assumptions about chloride is reasonably well justified in that there is a significant negative trend in concentration with distance from the source of Cl^-. MMHg (Figure 4B) also shows a decrease with distance from the ocean, however this trend does not quite satisfy our criteria for significance (p = 0.06). HgT mean concentrations with site distance are also decreasing (Figure 4C) but display only a weak tendency (p = 0.36). The possible reasons for this coastal-inland gradient are discussed in Section 3.4.

Table 3. Major ion analysis of fog water samples by site for 2014-2015. No SO_4^{2-} data from PPW are reported due to possible contamination from the DI rinse water which had elevated concentrations of SO_4^{2-} but not the other ions measured

Site ID	N	NH_4^+ (mg L^{-1})		Cl^- (mg L^{-1})		SO_4^{2-} (mg L^{-1})		NO_3^- (mg L^{-1})	
		mean	σ	mean	σ	mean	σ	mean	σ
HSU	12	2.01	1.60	18.58	25.16	34.19	45.90	4.90	8.33
PPW	26	2.20	1.66	1.41	2.23	--	--	4.68	4.48
BML	3	1.18	0.38	44.45	35.99	82.53	73.41	1.86	1.82
SFSU	2	2.29	0.37	3.16	0.90	6.69	1.09	3.70	1.84
UCSC	26	3.28	2.29	3.15	3.48	9.48	8.29	10.13	9.45
LML	6	2.56	1.09	53.88	83.76	88.22	134.55	6.96	7.97
FRF	10	2.63	0.93	7.74	12.64	15.63	21.91	9.17	8.90
All Sites 2014	42	2.65	2.06	7.00	14.03	15.72	26.77	6.84	8.19
All Sites 2015[a]	43	2.55	1.57	14.35	39.10	26.91	63.06	7.94	7.96

[a]No significant difference observed between 2014 and 2015 mean concentrations for any ions.

doi: 10.12952/journal.elementa.000101.t003

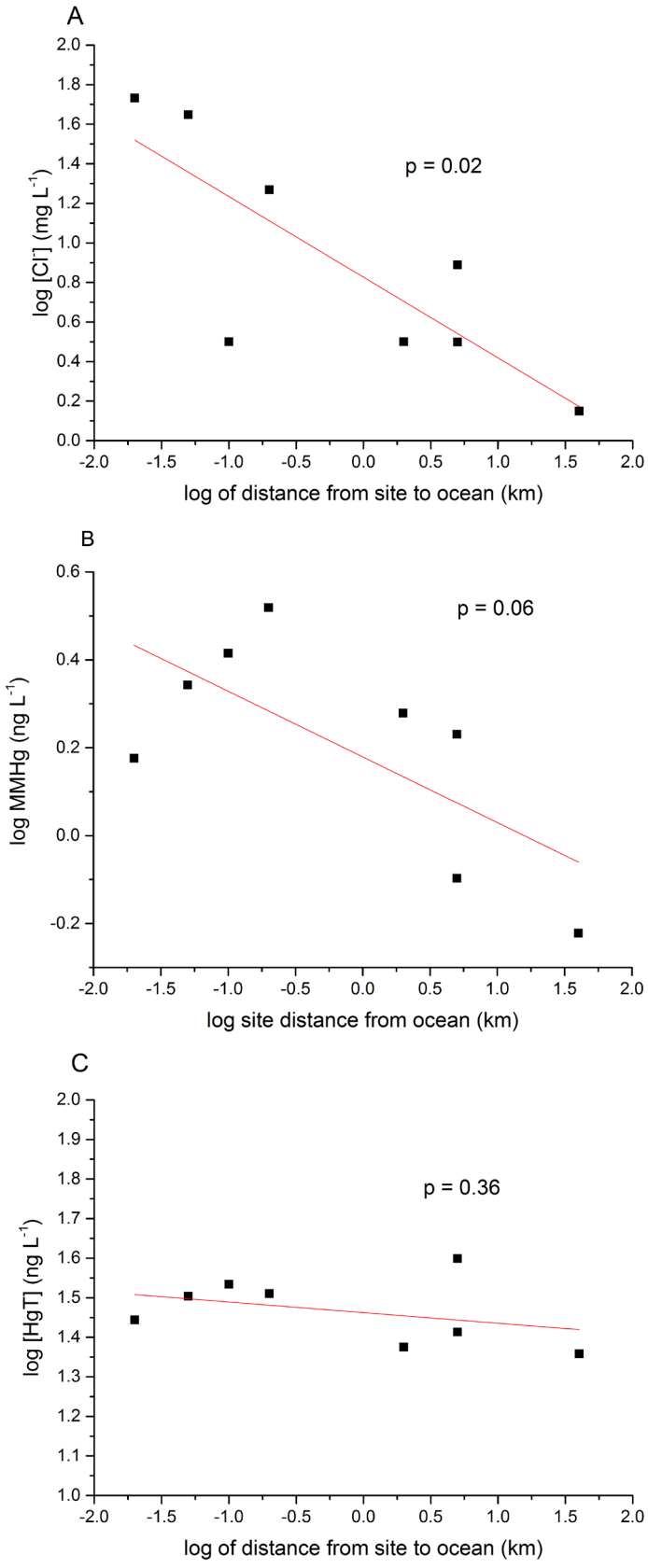

Figure 4

Log of mean A) Cl^-, B) MMHg and C) HgT concentration in fog water versus the log of each site's distance to the ocean (terrestrial sites only).

The p-values of linear fits are also shown.

doi: 10.12952/journal.elementa.000101.f004

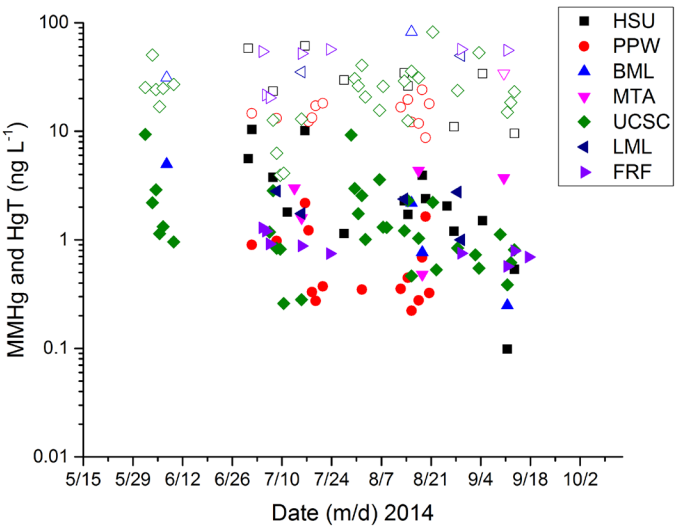

Figure 5

Monomethyl Hg (solid symbols) and total Hg (open symbols) concentrations in fog water taken from terrestrial sites indicated during 2014.

Note the log10 scale on the y-axis.

doi: 10.12952/journal.elementa.000101.f005

Temporal trends in fog water MMHg concentrations were also observed. Figure 5 shows the MMHg and HgT concentrations for each fog water sample taken over all terrestrial sites during 2014. A decrease in MMHg concentrations from higher in the early season (June) to lower in the later season (September) was observed. A Mann-Kendall trend test was performed on all fog water MMHg concentrations from 2014 and 2015 and for each terrestrial site individually (combining days with multiple samples into a daily mean) (Table S2). The results show that MMHg concentrations were trending significantly negative for all terrestrial sites combined ($p = 0.0002$) and for HSU, UCSC, and FRF individually for 2014 data. The trends were not significant in 2015 although the tendency was negative and had a p-value of 0.1. No significant trends were observed for HgT concentrations for 2014 or 2015 data. Also, no significant trends were observed in the field blank samples from either year (Figure S8) suggesting that the observed trend in MMHg in fog water samples was not a sampling nor analytical artifact.

The seasonal change in MMHg concentrations in fog water, seen especially in 2014, is consistent with a source of MMHg from coastal ocean upwelling of DMHg. Upwelling is driven by northerly winds that are typically at their peak in the spring and early summer along the California coast (Pennington and Chavez, 2000). Note however, that HgT shows no seasonal change, indicating that inorganic Hg in fog water may not be controlled by oceanic emissions but rather from oxidation of Hg^0 in the atmosphere as discussed in Section 3.4.

There was interannual variability observed in mean MMHg and HgT at the terrestrial sites with significantly higher concentrations of both species observed in 2014 compared to 2015. However, mean concentrations by year for the major ions NH_4^+, Cl^-, SO_4^{2-}, and NO_3^- were higher in 2015 than 2014 (Table 3), although none of these differences were significant. Overall, 2015 was less foggy than 2014 with about 25% fewer events and water volume collected with the CASCC (Table 2), but it is not known whether fog frequency or intensity played a role in the interannual variability in the mean concentrations of Hg species.

3.3 Interspecies correlations

Monomethyl Hg and HgT in fog water were not linearly correlated when data from all terrestrial sites were combined (Figure 6). At two sites, HSU and PPW, there were significant correlations between MMHg and HgT (Table 4), however at PPW the correlation was driven by one outlier sample (HgT = 170 ng L^{-1}) and no correlation was found with this sample removed. At HSU the slope ($\Delta MMHg/\Delta HgT$) was 0.13 ± 0.04.

Monomethyl Hg was found to be not correlated to any of the major ions measured in fog water from the three sites with sufficient data for a comparison (Table 4). Although mean MMHg concentrations by site were correlated with Cl^-, used here as a sea salt tracer (Figure 4), MMHg was not correlated with sea salt ions in individual fog samples. In contrast, HgT was significantly correlated with Cl^- at UCSC (6 km inland) and PPW (40 km inland) (Table 4). This is further discussed below.

3.4 Investigating the marine source of Hg species in fog

Figure 7 shows a working model of Hg cycling involving the ocean, atmosphere and land in the coastal marine environment. Depth profiles of DMHg concentrations measured off the coast of California as part of this project (Coale et al., 2015) show significantly higher concentrations in cyclonic eddies, which are mesoscale centers

Table 4. Linear correlation matricies (x vs. y) for chemical species measured in fog water 2014–2015 for sites with > 7 samples analyzed for all chemical species[a]

	HSU		PPW		UCSC	
x vs. y	HgT	MMHg	HgT	MMHg	HgT	MMHg
MMHg	**positive**	–	**positive**	–	NC	–
NH_4^+	**positive**	NC	NC	NC	NC	NC
Cl^-	NC	NC	**positive**	NC	**positive**	NC
SO_4^{2-}	NC	NC	NA	NA	**positive**	NC
NO_3^-	NC	NC	**positive**	NC	**positive**	NC

[a]Bold type indicates a significant linear correlation. NC denotes no significant correlation and NA denotes not applicable

doi: 10.12952/journal.elementa.000101.t004

of upwelling, than in anticyclonic eddies, which are mesoscale downwelling centers (Pegliasco et al., 2015). Many more eddies were present during the June cruises compared to those in August, reflecting the seasonal nature of upwelling. Concentrations of DMHg in surface ocean waters of the Monterey Bay are believed to be sufficient for a positive sea-air flux (Black et al., 2009). DMHg in the atmosphere would demethylate to MMHg via the reaction with the chlorine radical (Niki et al., 1983) (Reaction R8 in Figure 7) or we also suggest on marine aerosols at acidic pH due to the presence of methanesulfonic acid (Charlson et al., 1987) (Reaction R9). Our DMHg demethylation experiments (see Supplemental material) using surface sea water revealed loss rate constants of -0.08 hr^{-1} in the light and -0.05 hr^{-1} in the dark, corresponding to $\tau_{1/2}$ on the order of 6 to 10 hours suggesting this is a viable mechanism for decomposing marine DMHg to MMHg in fog (Coale et al., 2015). Since a lack of correlation between MMHg and Cl^- in fog water was observed (Table 4), this is consistent with DMHg demethylating in fog droplets as opposed to within sea salt aerosols.

Inorganic Hg, on the other hand, may enter fog water after being absorbed by sea salt aerosols, consistent with the observed correlations between HgT and Cl^- at two sites (Table 4). According to our conceptual diagram (Figure 7), the process begins with the oxidation of gaseous elemental Hg (Hg^0) in the presence of the bromine atom to form Hg^{II} compounds (Holmes et al., 2006, 2009) (Reactions R5–R7). Bromine atoms are formed in the atmospheric marine boundary layer (AMBL) through the activation of sea salt aerosol, where Br_2 is produced in a steady state reaction involving O_3 and HO_2 (Sander and Crutzen, 1996) (Reactions R1–R4). Gaseous Hg^{II} compounds are often very low (< 2 pg m^{-3}) in the AMBL (Zhang et al., 2012), in part because gaseous Hg^{II} has been observed to readily partition into the particulate phase due to uptake by sea salt aerosols (Malcolm et al., 2003). The positive correlation observed between HgT and Cl^- in fog water at two terrestrial sites in this study (Table 4) suggests that this is a likely source of HgT in fog.

Once in the fog droplet, MMHg could undergo photo-demethylation to inorganic Hg as has been observed in sea water (Monperrus et al., 2007; Black et al., 2009), rain water and simulated fog water (Bittrich et al., 2011). We wondered if this could account for the coastal-inland MMHg concentration gradient that was observed (Figure 4). Based on a previously published photo-demethylation rate constant in rain water (-0.022 hr^{-1}) (Bittrich et al., 2011), and an initial MMHg concentration of 2.2 ng L^{-1}, which was the mean value at the coastal site BML, the initial loss rate of MMHg in fog water was -0.048 ng L^{-1} h^{-1}. After

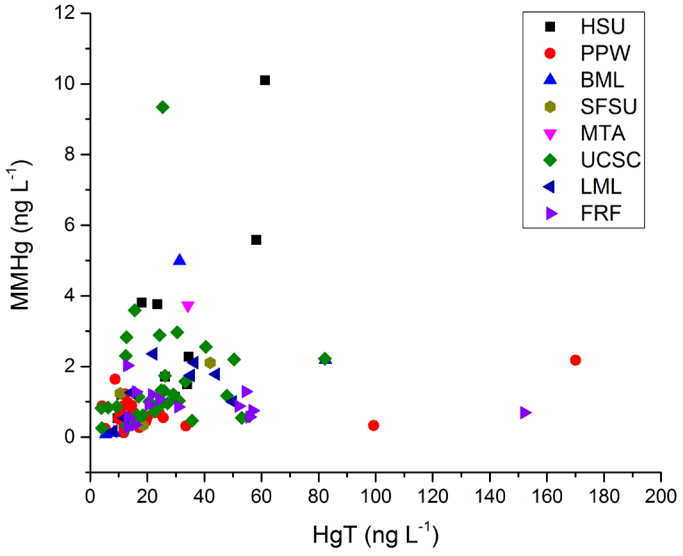

Figure 6
MMHg vs. HgT from fog water samples from all terrestrial sites 2014–2015.

Color and symbol scheme is the same as in Figure 5.

doi: 10.12952/journal.elementa.000101.f006

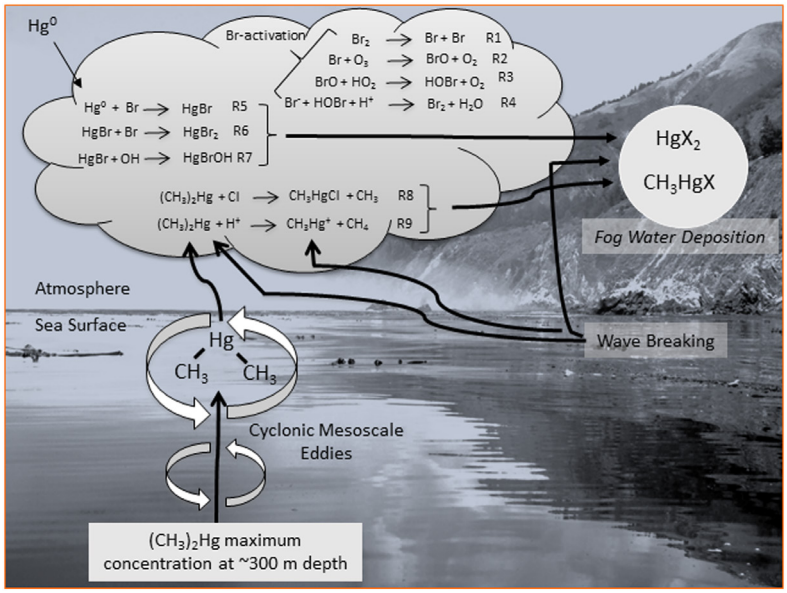

Figure 7

Conceptual diagram of the source of inorganic (HgX_2) and organic (CH_3HgX) in marine fog (Coale et al., 2015).

References for reactions R1–R9 are given in the text. Photo by Scott Gabara.

doi: 10.12952/journal.elementa.000101.f007

12 hours, an upper limit for the transport time between BML and PPW 40 km inland based on inspection of HYSPLIT back trajectories using the EDAS 40 km meteorological fields (Stein et al., 2015), this leaves 1.7 ng L^{-1} of MMHg in the fog water at PPW, greater than the observed mean MMHg which was 0.6 ng L^{-1}. Dark demethylation rates were essentially zero in rain water and simulated cloud water (Bittrich et al., 2011) suggesting that demethylation in the coastal California fog should be even slower than what was estimated using photo-demethylation rates since fog moves inland during the night. Thus, demethylation of MMHg appears to be too slow to account for the large differences seen between the coastal sites at BML and HSU and the inland site of PPW.

The coastal wave breaking zone may act as a source of MMHg in fog due to the potential for hydrophobic organic Hg compounds to become concentrated in the surface microlayer of the ocean, which is composed primarily of lipids and surfactants (Karavoltsos et al., 2015). Our data have shown that samples collected by the glass plate method for microlayer sampling (see Supplemental material) have MMHg concentrations far above the surface mixed layer (Coale et al., 2015). Wave breaking enhances the ventilation of methylated and inorganic Hg compounds to the atmosphere (Bayens et al., 1991) and could result in sites closest to the shore having the highest concentrations of Hg species as we have seen. However, fog over the ocean had low MMHg concentrations even though these location were also exposed to wind generated waves and rough sea state that likely mimicked wave action at the shore. More fog water samples will be needed from over the ocean and from right along the shore to investigate this hypothesis.

Once in the fog water, over 90% of the MMHg was in the particulate phase (< 0.45 μm) (Figure 8) suggesting that MMHg entered the fog in a particle or partitioned onto existing particles once in the bulk liquid. Measurements of MMHg in sub- and super-micron marine aerosols and of DMHg in the gas phase in the AMBL would be useful for tracking the source of MMHg in fog water (Gamberg et al., 2015; Baya et al., 2015).

3.5 Estimating the fog water flux of Hg species and comparison with the rain water flux

Daily fog water available for deposition per vertical square meter at each site, as outlined above and from here forward referred to more simply as "deposition", was determined by calculating the daily volumetric totals from each 1.00 m^2 SFC. This yielded a six-site mean (range) deposition of 0.10 ± 0.07 (0.02–0.21) of L m^{-2} d^{-1}. Annual fog water deposition was calculated by assuming that the daily fog water deposition extended for 180 days, the approximate length of the fog season (May–October). Daily mean rain water deposition per horizontal square meter was calculated by multiplying the average annual rainfall depth in Santa Cruz (730 mm or 0.73 m) (Conaway et al., 2010) by a 1.00 m^2 area giving a volume of 0.73 m^3 or 730 L, which fell during that rainy season of 180 days in duration (November–April) giving a daily deposition of 4 L m^{-2} d^{-1} (Table 5). Assuming that there is a parity between the vertically-oriented fog water deposition and the horizontal rain water capture, daily mean fog water deposition across six sites in this study comprised approximately 2.5% of the deposition from rain as measured in Santa Cruz in 2007. This result compares closely to the fog and rain data taken at a redwood forest site in Sonoma County, California by Ewing et al. (2009), who found that rain accounted for 98% of the throughfall water accumulation. Other studies in coastal

Table 5. Water, MMHg and HgT deposition fluxes for fog from this study (2014 data) and rain from Conaway et al. (2010)[a]

Calculated Quantity	Fog							Rain	Fog / Rain
	HSU	PPW	BML	UCSC	LML	FRF	Mean of 6 sites	Santa Cruz	
Water Deposition (L m^{-2} d^{-1})	0.09	0.21	0.15	0.02	0.05	0.09	0.10 ± 0.07	4.0 ± 0.1	0.025
Water Deposition (L m^{-2} yr^{-1})	17	39	27	3.0	9.0	17	19 ± 13	730 ± 24	0.025
MMHg conc. (ng L^{-1})	3.3	0.70	2.0	1.8	2.1	0.87	1.8 ± 0.9	0.14 ± 0.1	14
HgT conc. (ng L^{-1})	32.0	26.4	59.9	25.6	42.6	58.4	40.8 ± 15.5	5.8 ± 4.2	7.0
MMHg flux (ng m^{-2} yr^{-1})	56	23	59	5	13	13	34 ± 40	102 ± 76	0.33
HgT flux (ng m^{-2} yr^{-1})	544	877	860	79	249	668	546 ± 581	4230 ± 3180	0.13

[a]Because of the seasonal nature of both rain and fog in this region, 1 year was assumed to be equivalent to 180 days. Uncertainties on the flux of Hg species were calculated by propagation of error. Note that the rain water MMHg flux reported here was taken from Conaway et al. (2010) and represents a correction to what was published in Weiss-Penzias et al. (2012) which was erroneously reported as 9 ± 7 ng m^{-2} y-1.

doi: 10.12952/journal.elementa.000101.t005

California have reported widely varying fog water deposition from 0.02 L m^{-2} d^{-1} on Santa Cruz Island (Fischer and Still, 2007) to 15.6 L m^{-2} d^{-1} on Montara Mountain (Goodman, 1985). Interannual variability may also be large for fog deposition at any given site, as may be the presence or absence of foliar structures, which would translate fog water availability to actual fog water capture (Juvik et al., 2011). Multiyear observations of fog water deposition (unpublished data) collected at a site on the campus of California State University, Monterey Bay reveal that from 2009–2013 the mean fog water deposition to the SFC during August was 0.93 L m^{-2} d^{-1} but that for 2014–2015 the mean August fog water deposition to the SFC was only 0.12 L m^{-2} d^{-1}, close to the six-site mean reported above.

Fog water deposition multiplied by the mean concentrations of MMHg and HgT in fog water, results in the six-site mean depositional fluxes of 34 ± 40 and 546 ± 581 ng m^{-2} y^{-1}, respectively (Table 5). The value for MMHg is on the low end of that estimated previously (Weiss-Penzias et al., 2012) (14 to 1500 ng m^{-2} y^{-1}) mainly because fog water deposition rates in this study were on the low end of the range of values used in the previous calculations (0.04–4.8 L m^{-2} d^{-1}). The value for HgT flux is within the range published previously (Weiss-Penzias et al., 2012) (42 to 4600 ng m^{-2} y^{-1}). The proportion of fog to rain fluxes of MMHg and HgT is calculated to be 33% and 13%, respectively, making the fog water contribution to the wet deposition flux of Hg species in 2014, a small but a significant fraction.

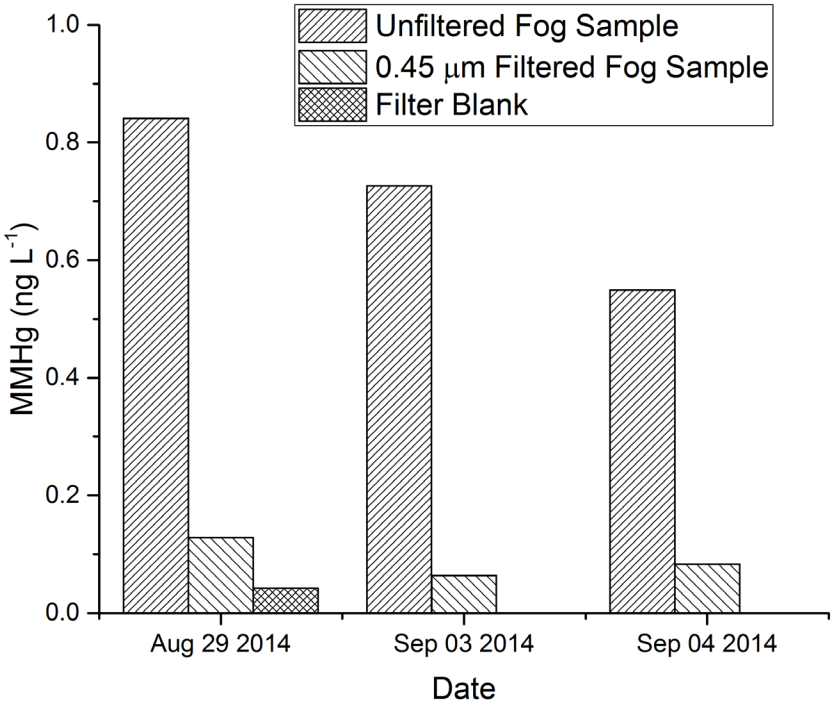

Figure 8

The effect of 0.45 μm filtration of fog water samples on MMHg concentrations.

The volume of fog water collected at the UCSC site was 220 mL, 125 mL, and 110 mL on Aug 29, Sep 3, and Sep 4, 2014, respectively, and these volumes were split into approximately equal aliquots one of which was filtered and other left unfiltered.

doi: 10.12952/journal.elementa.000101.f008

4.0 Conclusions

Marine fog water samples were collected over two summers at eight sites from Trinidad, California in the north to Marina, California in the south in addition to samples collected on four ship cruises off the coast of central and northern California during the summers of 2014 and 2015 (N = 149). The focus was on quantifying MMHg and HgT concentrations in fog water and observing spatial and temporal trends that would help elucidate the source of MMHg in fog. Mean concentrations across all terrestrial sites for both years of MMHg and HgT were 1.6 ± 1.9 ng L^{-1} and 27.6 ± 25.8 ng L^{-1}, respectively. Rain water samples obtained in this work with the same sampler used for fog (CASCC) and in previous research using an open funnel at a site in Santa Cruz, California contained an order of magnitude lower MMHg concentrations (~0.15 ng L^{-1}). MMHg in rain collected in this study was 1.4% of HgT, whereas MMHg in fog from this study was 5.8% (range of site means: 2.0–10.8%) of HgT. In contrast, fog water collected over the ocean in this study had a mean MMHg concentration of 0.08 ± 0.15 ng L^{-1} (0.4% of HgT). Thus, an interesting pattern emerged with fog water over the land containing significantly higher concentrations of MMHg compared to rain water over the land and fog water over the ocean.

Spatial trends of MMHg and HgT concentrations in fog water collected at the terrestrial sites showed decreasing tendencies with site distance from the ocean ($p = 0.06$ and $p = 0.37$, respectively). Mean MMHg concentrations varied from 2.2 ng L^{-1} at the coastal site BML to 0.6 ng L^{-1} at the site PPW 40 km inland. Applying a photo-demethylation rate constant of -0.022 hr^{-1}, which was observed in rain water in a previous study and a transport time of 12 hours from coastal BML to inland PPW, gave a predicted MMHg concentration of 1.7 ng L^{-1} at PPW, ~3 times higher than the observed concentration at this site. This suggests that demethylation is not likely fast enough to account for the observed coastal-inland gradient. Furthermore, since dark demethylation is even slower or does not occur at all and much of fog transport is at night, the loss of MMHg calculated here likely represents an upper limit of the amount lost due to demethylation.

The relatively low concentrations of MMHg in fog collected at sea and the coastal-inland gradients of decreasing MMHg concentration from BML-PPW and from LML-FRF can be explained if a major source of MMHg in fog is from the immediate coastline due breaking waves which might aerosolize hydrophobic organic Hg compounds which tend to be enriched in the surface microlayer of near-shore water, as was observed in this work. Fog over the ocean having low MMHg concentrations would tend to dilute fog from the immediate coastline with higher MMHg concentrations resulting in a sharp fall-off in MMHg concentrations with distance inland, as was observed in the low MMHg concentrations at PPW and FRF. However, more samples will need to be taken in the off-shore to near shore and inland environments in order to validate this hypothesis, in addition to performing photo-demethylation experiments on fog water to see whether the rate constants are comparable to those determined for rain water.

Estimates of the fog water flux of MMHg and HgT were obtained by multiplying the mean fog water deposition to the SFC from six sites by the mean fog water concentrations of the Hg species. The result is a six-site mean fog water MMHg and HgT flux for the year 2014 of 34 ± 40 ng m^{-2} y^{-1} and 546 ± 581 ng m^{-2} y^{-1}, respectively. These values are 33% and 13% of the rain water flux of MMHg and HgT, respectively, for 2007–2008 in Santa Cruz. Overall, fog water deposition was low in summers of 2014 and 2015, which led to calculated fog water fluxes of MMHg and HgT that were lower than previous estimates.

References

Baya P, Gosselin M, Lehnherr I, St. Louis V, Hintelmann H. 2015. Determination of monomethylmercury and dimethylmercury in the Arctic marine boundary layer. *Environ Sci Technol* **49**: 223–232. doi: 10.1021/es502601z.

Bayens W, Leermakers M, Dedeurwaerder H, Lansens P. 1991. Modelization of the mercury fluxes at the air-sea interface. *Water Air Soil Pollut* **56**: 731–744.

Bittrich DR, Rutter AP, Hall BD, Schauer JJ. 2011. Photodecomposition of methylmercury in atmospheric waters. *Aerosol AirQual Res* **11**: 290–298.

Black FJ, Conaway CH, Flegal AR. 2009. Stability of dimethylmercury in seawater and its conversion to monomethylmercury. *Environ Sci Technol* **43**: 4056–4062.

Bloom N. 1989. Determination of picogram levels of methylmercury by aquieous phase ethylation, followed by cryogenic gas chromatography with cold vapour atomic fluorescence detection. *Can J Fish Aquatic Sci* **46**: 1131–1140.

Bloom NS, Watras CJ. 1989. Observations of methylmercury in precipitation. *Sci Total Environ* **87–88**: 199–207.

Carrillo JH, Emert SE, Sherman DE, Herckes P, Collett JL. 2008. An economical optical cloud/fog detector. *Atmos Res* **87**: 259–267.

Charlson RJ, Lovelock J, Andreae M, Warren S. 1987. Oceanic phytoplankton, atmospheric sulphur, cloud albedo and climate. *Nature* **326**: 655–661.

Coale K, Heim W, Olsen A, Chiswell H, Byington A, et al. 2015. Dimethylmercury in seawater: A potential source of monomethylmercury in fog. *American Geophysical Fall Meeting*. San Francisco: B11D-0466.

Collett JL, Bator A, Sherman DE, Moore KF, Hoag KJ, et al. 2002. The chemical composition of fogs and intercepted clouds in the United States. *Atmos Research* **64**: 29–40.

Conaway CH, Black FJ, Gault-Ringold M, Pennington JT, Chavez FP, et al. 2009. Dimethylmercury in coastal upwelling waters, Monterey Bay, California. *Environ Sci Technol* **43**: 1305–1309.

Conaway CH, Black FJ, Weiss-Penzias P, Gault-Ringold M, Flegal AR. 2010, Mercury speciation in Pacific coastal rainwater, Monterey Bay, California. *Atmos Environ* **44**: 1788–1797.

Demoz BB, Collett Jr JL, Daube Jr BC. 1996. On the Caltech active strand cloudwater collectors. *Atmos Res* **41**: 47–62.

Driscoll CT, Mason RP, Man Chan H, Jacob DJ, Pirrone N. 2013. Mercury as a global pollutant: Sources, pathways, and effects. *Environ Sci Technol* **47**: 4967–4983. doi: 10.1021/es305071v.

Ewing HA, Weathers KC, Templer PH, Dawson TE, Firestone MK, et al. 2009. Fog water and ecosystem function: Heterogeneity in a California redwood forest. *Ecosystems* **12**: 417–433. doi: 10.1007/s10021-009-9232-x.

Fischer DT, Still CJ. 2007. Evaluating patterns of fog water deposition and isotopic composition on the California Channel Islands. *Water Resour Res* **43**: W04420. doi: 10.1029/2006WR005124.

Fitzgerald WF, Engstrom DR, Mason RP, Nater EA. 1998. The case for atmospheric mercury contamination in remote areas. *Environ Sci Technol* **32**: 1–7.

Gamberg M, Chételat J, Poulain AJ, Zdanowicz C, Zheng J. 2015. Mercury in the Canadian Arctic terrestrial environment: An update. *Sci Total Environ* **509–510**: 28–40.

Gardfeldt K, Munthe J, Stromberg D, Lindqvist O. 2003. A kinetic study on the abiotic methylation of divalent mercury in the aqueous phase. *Sci Total Environ* **304**: 127–136. doi: 10.1016/S0048-9697(02)00562-4.

Gill GA, Fitzgerald WF. 1987. Picomolar mercury measurements in seawater and other materials using stannous chloride reduction and two-stage gold amalgamation with gas phase detection. *Mar Chem* **20**: 227–243.

Goodman J. 1985. The collection of fog drip. *Water Resour Res* **21**: 392–394.

Gratz LE, Keeler GJ, Morishita M, Barres JA, Dvonch JT. 2013. Assessing the emission sources of atmospheric mercury in wet deposition across Illinois. *Sci Total Environ* **448**: 120–131.

Hammerschmidt CR, Lamborg CH, Fitzgerald WF. 2007. Aqueous phase methylation as a potential source of methylmercury in wet deposition. *Atmos Environ* **41**: 1663–1668. doi: 10.1016/j. atmosenv.2006.10.032.

Harris RC, Rudd JWM, Amyot M, Babiarz CL, Beaty KG, et al. 2007. Whole-ecosystem study shows rapid fish mercury response to changes in mercury deposition. *P Natl Acad Sci* **104**: 16586–16591. doi: 10.1073/pnas.0704186104.

Helsel DR, Mueller DK, Slack JR. 2006. Computer program for the Kendall family of trend tests. *U.S. Geological Survey Scientific Investigations Report 2005–5275*.

Holmes C, Jacob D, Mason R, Jaffe DA. 2009. Sources and deposition of reactive gaseous mercury in the marine atmosphere. *Atmos Environ* **43**: 2278–2285. doi: 10.1016/j.atmosenv.2009.01.051, 2009.

Holmes C, Jacob D, Yang X. 2006. Global lifetime of elemental mercury against oxidation by atomic bromine in the free troposphere. *Geophys Res Lett* **33**: L20808. doi: 10.1029/2006GL027176.

Horvat M, Liang L, Bloom NS. 1993. Comparison of distillation with other current isolation methods for the determination of methyl mercury compounds in low level environment samples. *Anal Chim Acta* **282**: 153–168.

Johnstone JA, Dawson TE. 2010. Climatic context and ecological implications of summer fog decline in the coast redwood region. *P Natl Acad Sci*. doi: 10.1073/pnas.0915062107.

Juvik JO, DeLay JK, Kinney KM, Hansen EV. 2011. A 50th Anniversary reassessment of the seminal 'Lanai'i fog drip study' in Hawai'i. *Hydrol Process* **25**: 402–410. doi: 10.1002/hyp.7803.

Karavoltsos S, Kalambokis E, Sakellari A, Plavšić M, Dotsika E, et al. 2015. Organic matter characterization and copper complexing capacity in the sea surface microlayer of coastal areas of the Eastern Mediterranean. *Mar Chem* **173**: 234–243.

Kieber RJ, Parler NE, Skrabal SA, Willey JD. 2008. Speciation and photochemistry of mercury in rainwater. *J Atmos Chem* **60**: 153–168. doi: 10.1007/s10874-008-9114-1.

Koracin D, Dorman CE, Lewis JM, Hudson JG, Wilcox EM, et al. 2014. Marine fog: A review. *Atmos Res* **143**: 142–175.

Laskin A, Moffet RC, Gilles MK, Fast JD, Zaveri RA, et al. 2012. Tropospheric chemistry of internally mixed sea salt and organic particles: Surprising reactivity of NaCl with weak organic acids. *J Geophys Res* **117**: D15302. doi: 10.1029/2012JD017743.

Lindberg S, Bullock R, Ebinghaus R, Engstrom D, Feng X, et al. 2007. A synthesis of progress and uncertainties in attributing the sources of mercury in deposition. *Ambio* **36**: 19–32.

Lynam MM, Dvonch JT, Hall NL, Morishita M, Barres JA. 2014. Spatial patterns in wet and dry deposition of atmospheric mercury and trace elements in central Illinois, USA. *Environ Sci Pollut Res* **21**: 4032–4043. doi: 10.1007/s11356-013-2011-4.

Malcolm EG, Keeler GJ, Landis MS. 2003. The effects of the coastal environment on the atmospheric mercury cycle, *J Geophys Res* **108**(D12): 4357. doi: 10.1029/2002JD003084.

Manders AM, Schaap M, Querol X, Albert MF, Vercauteren J, et al. 2010. Sea salt concentrations across the European continent. *Atmos Environ* **44**: 2434–2442.

Mason RP, Choi AL, Fitzgerald WF, Hammerschmidt CR, Lamborg CH, et al. 2012. Mercury biogeochemical cycling in the ocean and policy implications. *Environ Res* **119**: 101–117.

Mason RP, Vandal GM, Fitzgerald WF. 1992. The sources and composition of mercury in Pacific Ocean rain. *Atmos Chem* **14**: 489–500.

Mergler D, Anderson HA, Chan LHM, Mahaffey KR, Murray M, et al. 2007. Methylmercury exposure and health effects in humans: A worldwide concern. *Ambio* **36**(3). doi: 10.1579/0044-7447.

Monperrus M, Tessier E, Amouroux D, Leynaert A, Huonnic P, et al. 2007. Mercury methylation, demethylation and reduction rates in coastal and marine surface waters of the Mediterranean Sea. *Mar Chem* **107**: 49–63.

Munthe J, Kindbom K, Kruger O, Petersen G, Pacyna J, et al. 2001. Examining source-receptor relationships for mercury in Scandinavia. *Water Air Soil Pollut: Focus* **1**: 299–310.

Niki H, Maker PD, Savage CM, Breitenbach LP. 1983. A fourier transform study of the kinetics and mechanism for the reaction Cl + CH,HgCH. *J Phys Chem* **87**: 3722–3723.

Ortiz C, Weiss-Penzias P, Fork S, Flegal AR. 2014. Total and monomethylmercury in terrestrial arthropods from the central California coast. *Bull Environ Contam Toxicol* **94**: 425–430.

Parker JL, Bloom NS. 2005. Preservation and storage techniques for low-level aqueous mercury speciation. *Sci Total Environ* **337**: 253–263. doi: 10.1016/j.scitotenv.2004.07.006.

Pegliasco C, Chaigneau A, Morrow R. 2015. Main eddy vertical structures observed in the four major eastern boundary upwelling systems. *J Geophys Res-Oceans* **120**: 6008–6033. doi: 10.1002/2015JC010950.
Pennington JT, Chavez FP. 2000. Seasonal fluctuations of temperature, salinity, nitrate, chlorophyll and primary production at station H3/M1 over 1989–1996 in Monterey Bay, California. *Deep-Sea Res Pt II* **47**(5–6): 947–973.
Pirrone N, Aas W, Cinnirella S, Ebinghaus R, Hedgecock IM, et al. 2013. Toward the next generation of air quality monitoring: Mercury. *Atmos Environ* **80**: 599–611.
Sander R, Crutzen PJ. 1996. Model study indicating halogen activation and ozone destruction in polluted air masses transported to the sea. *J Geophys Res* **101**: 9121–9138.
Sawaske SR, Freyburg DL. 2015. Fog, fog drip, and streamflow in the Santa Cruz Mountains of the California Coast Range. *Ecohydrology*. doi: 10.1002/eco.1537.
Schemenauer RS, Cereceda P. 1994. A proposed standard fog collector for use in high-elevation regions. *J Appl Meteorol* **33**.
Scheuhammer AM, Meyer MW, Sandheinrich MB, Murray MW. 2007. Effects of environmental methylmercury on the health of wild birds, mammals, and fish. *Ambio* **36**: 12–18.
Schroeder WH, Munthe J. 1998. Atmospheric mercury – An overview. *Atmos Environ* **32**: 809–822.
Shanley JB, Engle MA, Scholl M, Krabbenhoft DP, Brunette R, et al. 2015. High mercury wet deposition at a "clean air" site in Puerto Rico. *Environ Sci Technol* **49**: 12474–12482.
St. Louis VL, Hintelman H, Graydon JA, Kirk JL, Barker J, et al. 2007. Methylated mercury species in Canadian high Arctic marine surface waters and snowpacks. *Environ Sci Technol* **41**: 6433–6441. doi: 10.1021/es070692s.
St. Louis VL, Sharp MJ, Steffen A, May A, Barker J, et al. 2005. Some sources and sinks of monomethyl and inorganic mercury on Ellesmere Island in the Canadian High Arctic. *Environ Sci Technol* **39**: 2686–2701.
St. Pierre KA, St. Louis VL, Kirk JL, Lehnherr I, Wang S, et al. 2015. Importance of open marine waters to the enrichment of total mercury and monomethylmercury in lichens in the Canadian High Arctic. *Environ Sci Technol* **49**: 5930–5938. doi: 10.1021/acs.est.5b00347.
Steffen A, Lehnherr I, Cole A, Ariya P, Dastoor A, et al. 2015. Atmospheric mercury in the Canadian Arctic. Part I: A review of recent field measurements. *Sci Total Environ* **509–510**: **3**–15.
Stein AF, Draxler RR, Rolph GD, Stunder BJB, Cohen MD, et al. 2015. NOAA's HYSPLIT atmospheric transport and dispersion modeling system. *B Am Meteorol Soc* **96**: 2059–2077. doi: 10.1175/BAMS-D-14-00110.1.
UNEP Minamata Convention. 2014. UNEP Minamata Convention on Mercury. http://www.mercuryconvention.org/.
USEPA. 2001. Guidance for Implementation and Use of EPA Method 1631 for the Determination of Low-Level Mercury (40 CFR part 136). *821-R-01-023*. United States Environmental Protection Agency.
USEPA. 2002. Method 1631, Revision E: Mercury in Water by Oxidation, Purge and Trap, and Cold Vapor Atomic Fluorescence Spectrometry. *821-R-02-019*. United States Environmental Protection Agency.
Weathers KC, Lovett GM, Likens GE, Caraco NF. 2000. Cloudwater inputs of nitrogen to forest ecosystems in southern Chile: Forms, fluxes, and sources. *Ecosystems* **3**: 590–595.
Weiss-Penzias PS, Ortiz C, Acosta RP, Heim W, Ryan JP, et al. 2012. Total and monomethyl mercury in fog water from the central California coast. *Geophys Res Lett* **39**(3).
Zhang Y, Jaeglé L, van Donkelaar A, Martin RV, Holmes CD, et al. 2012. Nested-grid simulation of mercury over North America. *Atmos Chem Phys* **12**: 6095–6111.

Contributions

- Contributed to conception and design: PWP, KC, WH, DF
- Contributed to acquisition of data: All authors
- Contributed to analysis and interpretation of data: PWP, KC, WH, DF
- Drafted and/or revised the article: PWP, KC, WH, DF
- Approved the submitted version for publication: All authors

Acknowledgments

We would like to thank: Chad Saltikov, Rob Franks, Jim Velzy, Dave Thayer, Joe Cox, Jeremiah Tsyporin, Kona Orlandi, Isaac Bakerman, Ossian Sahba, Scott Conrad, Randolf Skrovan, John Ryan, Lelia Hawkins, Alexander Mairs, Matthew Bowman, Mitch Gravelle, Summer Wilson, Thomas Barkley, Christopher Eljenholm, Erin Coffey, James Gongola, Gabriel Griffiths, Mike Porter, Alicia Torregrosa, Holly Chiswell, Amy Byington, Adam Newman, John Negrey, Stephen Martenuk, Chris Beebe, Autumn Bonnema, April Sjoboen Guimarães, Dave Anderson, Jeff Weiss, and the captains and crews of the R/V Pt. Sur, R/V Sproul, and R/V Oceanus.

Funding information

This project was funded by the National Science Foundation award # OCE-1333738.

Competing interests

The authors do not have any competing interests.

Supplemental material

- **Table S1. Field blank results for HgT and MMHg.**
  Mean concentrations, standard deviations, and number of valid and invalid field blank rinse water samples by site for the 2014 and 2015 campaigns. Blank was valid if [MMHg]blank / [MMHg]fog sample < 0.2. Mean sample values were calculated based on the data in Table 2. (DOC) doi: 10.12952/journal.elementa.000101.s001
- **Table S2. Mann-Kendall trend analysis of MMHg.**
  Mann-Kendall time-trend analysis on MMHg concentrations in fog water by year for sites with at least 15 samples total. Statistically significant trends are shown in bold. (DOC) doi: 10.12952/journal.elementa.000101.s002

- **Text S1. Details on shipboard fog sampling and seawater experiments.**
  This section describes the mounting configurations, operational methodologies and tactical sampling considerations for the at-sea fog water sampling during this program. Also described are the acid incubation and microlayer measurements of MMHg. (DOC) doi: 10.12952/journal.elementa.000101.s003
- **Figure S1. The Caltech Active Strand Cloudwater Collector (CASCC).**
  The UCSC built CASCC. (DOC) doi: 10.12952/journal.elementa.000101.s004
- **Figure S2. The standard 1 m^2 passive fog collector.**
  The standard fog collector with the Chilean Raschel mesh and the Spectrum® tipping bucket rain gauge and data logger. (DOC) doi: 10.12952/journal.elementa.000101.s005
- **Figure S3. The CASCC deployed on the R/V Pt. Sur.**
  Shipboard fog water sampling on the R/V Pt. Sur. The collector has front and back doors hanging down and is at a height of 11 m. (DOC) doi: 10.12952/journal.elementa.000101.s006
- **Figure S4. The CASCC deployed on the R/V Sproul.**
  Fog water sampling on the R/V *Robert Gordon Sproul*. This location made it easier to access and clean the CASCC, but was not as isolated from the ship's exhaust. (DOC) doi: 10.12952/journal.elementa.000101.s007
- **Figure S5. Laboratory intercomparison for MMHg.**
  Two-laboratory (UCSC and MLML) intercomparison of MMHg concentrations in fog water collected at HSU on the dates shown. (DOC) doi: 10.12952/journal.elementa.000101.s008
- **Figure S6. Laboratory intercomparison for HgT.**
  Figure S-6: Two-laboratory (UCSC and MLML) intercomparison of HgT concentrations in fog water collected at UCSC on the dates shown. (DOC) doi: 10.12952/journal.elementa.000101.s009
- **Figure S7. Laboratory intercomparison for SO_4^{2-} and NO_3^-.**
  Laboratory intercomparison (UCSC and Harvey Mudd (HM)) of SO_4^{2-} and NO_3^- concentrations in fog and field blank water collected at the UCSC site. (DOC) doi: 10.12952/journal.elementa.000101.s010
- **Figure S8. Field blanks concentrations of HgT and MMHg at all land sites.**
  HgT (open symbols) and MMHg (closed symbols) in field blank rinse water samples from all collection sites in 2014–2015, all samples. (DOC) doi: 10.12952/journal.elementa.000101.s011

Data accessibility statement

Concentrations of analytes measured in fog water are stored on a UC Santa Cruz computer and are available for use by contacting the corresponding author.